



Обзорная статья • Review article

УДК 553.62

DOI: 10.19110/geov.2022.9.1

Genetic types of corundum

V. V. Shchiptsov^{1, 2}, N. G. Barnov³¹Institute of Geology, Karelian Research Centre, RAS, Petrozavodsk²Petrozavodsk State University, Petrozavodsk; vv.shchiptsov@gmail.com³Mining Institute, National Research University «MISIS», Moscow; barnov@inbox.ru

It is pointed out that corundum is the only natural modification with corundum Al and O packing motif, which determines the physical and chemical features of noble corundum. Based on the authors' ideas about the genesis of noble corundum with the application of original analytical data, which clarify the consolidated literature data, corundums of the magmatic, metamorphic and detrital series are defined. A scheme of the location of the main deposits of noble corundums of the world is given. It is stated that all properties of noble corundums are determined by their primary indigenous origin. The general condition of corundum formation is protocrystallization from melts in deep magmatic centers under the condition of subsequent rapid solidification of the main mass of the melt. The presented research methods allow determining characteristics and a wide range of application of corundums. Precambrian corundum deposits are of the prevailing genetic type.

Keywords: *noble corundum, genesis, magmatism, metamorphism, Precambrian.*

Генетические типы корундов

В. В. Щипцов^{1, 2}, Н. Г. Барнов³¹Институт геологии КарНЦ РАН, ФИЦ «Карельский научный центр РАН», Петрозаводск²Петрозаводский государственный университет, Петрозаводск³Горный институт НИТУ «МИСиС», Москва

Показано, что корунды представляют собой единственную природную модификацию с корундовым мотивом упаковки Al и O и что определяет физические и химические особенности благородных корундов. На основании авторских представлений о генезисе благородных корундов с приложением оригинальных аналитических данных, уточняющих сводные литературные данные, выделены корунды магматогенной, метаморфогенной и детритовой серий. Дана схема размещения основных месторождений благородных корундов мира. Приведены методики исследований, позволяющие определить характеристики и широкий диапазон областей использования корундов. Месторождения корундов докембрая относятся к превалирующему генетическому типу.

Ключевые слова: *благородные корунды, генезис, магматизм, метаморфизм, докембрий.*

Introduction

In the introductory part of the article, the authors give a brief overview of corundum.

Corundum is the only natural modification with corundum packing motif of Al and O atoms. Its crystals are distinguishable by their hardness, colour and shade.

All varieties of corundum, including gem varieties (ruby and sapphire), crystallize in the ditrigonal-scaleno-hedral form of trigonal syngony symmetry. The refractive indices of corundum are constant with Ne values of 1.760 – Ne 1.768. B. W. Andersen and C. J. Paune [1] proposed to use the specific gravity of gem corundum as a reference.

The density of most gem varieties is 3.96–3.99 g/cm³, reaching 4.4.1 for green and blue-green sapphires from Australia. The mineral has a hardness of 9 on the Mohs scale and is the second only to diamond.

Corundum has the chemical composition of Al₂O₃ typically containing trace amounts of iron, titanium, chromium, and vanadium. Inclusions of rutile, hematite, ilmenite, garnet and spinel can be present.

The idiochromatic colouring of gemstones is caused by transition metal ions: Fe, Co, Ni, Mn, C, Cr, V, and Ti.

They are capable of absorbing a certain wavelength in the visible spectrum, thus determining colour. Ruby and sapphire contain 5 of these elements – Cr, V, Ti, Fe, Mn – as impurities.

The goal of this paper is to present the author's view on the genesis of noble corundums supported by the original analytical data and data already existing in the literature.

Corundum-bearing formations of the world

Geological and petrological conditions of corundum crystallization are diverse [2, 3, 6, 21, 23, 25–27, 29, 33, 36, 37, 40]. Deposits of noble corundums (rubies and sapphires) have been identified in the places, where their formation is associated with specific growth conditions of transparent crystals.

Rubies and sapphires are extracted mainly from the placers formed on the slopes and valleys of rivers, where the primary bedrock deposits were destroyed and corundum, as a mineral extremely resistant to mechanical and chemical attack, moved into sand/gravel river (more rare-

For citation: Shchiptsov V. V., Barnov N. G. Genetic types of corundum. Vestnik of Geosciences, 2022, 9(333), pp. 3–14, doi: 10.19110/geov.2022.9.1.

Для цитирования: Щипцов В. В., Барнов Н. Г. Генетические типы корундов // Вестник геонаук. 2022. 9(333). С. 3–14. DOI: 10.19110/geov.2022.9.1.



ly lake and marine) sediments. Such deposits are economically viable owing to the possibility of mineral extraction through simple operations of sieving or washing [7–9].

Alluvial, deluvial-alluvial placers and eluvial, eluvial-deluvial residual deposits of ancient weathering are of primary importance in the total balance of gem corundums production [10–15]. The primary ruby- and sapphire-bearing bodies, due to which the secondary deposits are formed, have been insufficiently studied.

The layout below (Fig. 1) shows the main deposits of noble corundums in the world.

Based on the international genetic classification of world noble corundums [6], we divide corundums into types and subtypes. The magmatic series (type I) includes alkaline basalts (IA subtype) and kimberlites (IB subtype). These subtypes have no industrial significance and are considered by us as necessary taxa in the general taxonomy. The rocks have undergone metamorphism of amphibolite, granulite or eclogite facies conditions.

The metamorphosed series includes two types – type IIA metamorphic sensu stricto and type IIB metamorphic-metasomatic. Type IIA has two subtypes: subtype II A1

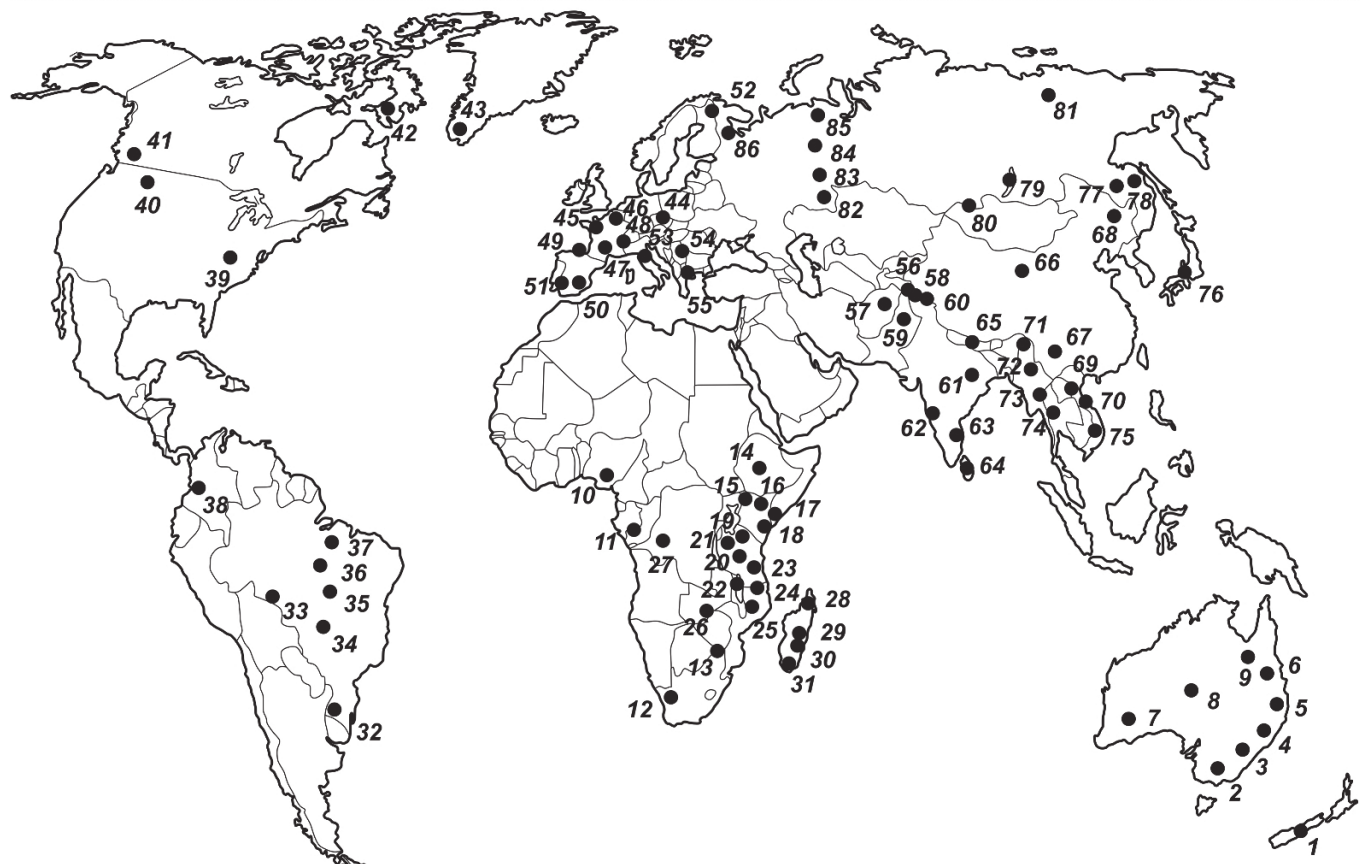


Fig. 1. Layout of the main corundum-bearing areas, deposits and large corundum occurrences of the world.

New Zealand: 1 – Westland (Hokitika); Australia: 2 – West Melbourne fields, 3 – Tumbarumba, 4 – Macquarie-Cudgegong, Barrington Tops-Yarrowitch, 5 – New England fields (Inverell). 6 – Anakie fields-Rubyvale. 7 – Poona, 8 – Harts range, 9 – Lava Plains; Nigeria: 10 – Kaduna; Congo: 11 – Kinshasa; South Africa: 12 – Namakvaland, 13 – Barberton; Ethiopia: 14 – Kibre mengist, Dilla; Kenya: 15 – West Pokot, 16 – Baringo, 17 – Kitui. 18 – Mangare (Rockland-former John Saul mine; Penny Lane; Aqua, Hard Rock; Tanzania: 19 – Umbo valley, 20 – Longido, Losogonoi, 21 – Winza, Loolera (Kibuko), 22 – Morogoro (Mwalazi; Visakazi; Nyama, Kibuko), Mahenge (Lukande; Mayote; Kitwalo; Ipango), 23 – Songea, 24 – Tunduru; Mozambique: 25 – Montepuez (Namahumbire/Namahaca), M'sawize, Ruambeze; Zimbabwe: 26 – O'Briens (Verdits); Democratic Republic of Congo: 27 – Mbaji-Mayi; Madagascar: 28 – Andilamena, Ambodivoangy-Zahamena, Didy, Vatomandry, 29 – Andriba; Ankaratra (Antsirabe-Antanifotsy region, Soamiakatra-Ambohimandroso; Ambohibary), 30 – Ambositra, Ihosy, Zazafotsy, Ilakaka-Sakaraha; 31 – Bekily-Vohibory area (Ambatomena; Ianapera; Fotadrevo; Anavoha; Maniry; Gogogogo; Vohitany; Ejeda); Brazil: 32 – State Santa Katerina, Byra-Velha, 33 – State Mato Grosso de Sul, 34 – State San Paulu, Itaka, 35 – State Minas Gerais, 36 – State Goias, 37 – State Bahia; Colombia: 38 – Mercaderes-Rio Mayo; USA: 39 – North Carolina (Corundum Hill; Cowee Valley; Buck Creek, Rock Creek), 40 – Cone Valley; Canada: 41 – Revelstoke. 42 – Baffin Island; Greenland: 43 – South of Nuuk region (Fiskenasset district-Aappaluttoq); North of Nuuk (Stove; Kangerdluarssuk); Switzerland: 44 – Campo Lungo; France: 45 – Brittany (Champtoceaux), 46 – French Massif Central (Haut-Allier-Chantel; Peygerolles; Lozire-Aveyron-Marvejols), 47 – Vialat-du-Tarn, 48 – Pyrenees (Arignac); Spain: 49 – Alboran sea, 50 – Marrocos, 51 – Beni Bousera; Norway: 52 – Froland; Italy: 53 – Piedmont; Macedonia: 54 – Prilep; Greece: 55 – Gorgona-Xanthi, Paranesti-Drama; Tajikistan: 56 – Snejzhnoe, Turakuloma, Badakhshan; Afghanistan: 57 – Jegdalek, Kash; Pakistan: 58 – Hunza valley, 59 – Batakundi, Nangimali, 60 – Dir; India: 61 – Orissa, Kalahandi, 62 – Karnakata (Mysore), 63 – Andhra Pradesh (Salem district); Sri Lanka: 64 – Ratnapura, Polonnaruwa, Elahera; Nepal: 65 – Chumar, Ruyil; China: 66 – Sichuan and Yannan, 67 – Qinghai, 68 – Yuan Jiang; Vietnam: 69 – Luc Yen-Yen Bai; 70 – Quy Chau; Myanmar: 71 – Mogok, 72 – Namyu, 73 – Mong Hsu; Thailand: 74 – Chanthaburi-Trat (BoWaen, Bo NaWong, Wat Tok Phrom, Bo Rai, Nong Bon); Cambodia: 75 – Pailin, Samlaut; Japan: 76 – Ida; Russia: 77 – Primorie, the Pervomaiskoe occurrence, 78 – Nezametninskoe deposit, Khabarovsk Territory, 79 – Budunskoe



deposit, Lake Baikal; 80 — Tuva, Khansungsky occurrence; 81 — Yakutia, Neryuga, Chaynytskoe deposit; 82 — Cherry Mountains; 83 — Southern Ural, Borzovsky placer; 84 — Ilmensky mountains; Middle Ural, Kornilov-Log; 85 — Makar-Ruz; 86 — Khitostrov

Рис. 1. Схема размещения основных корундоносных областей, месторождений и крупных проявлений корундов мира. Новая Зеландия: 1 — Westland (Hokitika); Австралия: 2 — West Melbourne fields, 3 — Tumbarumba, 4 — Macquarie-Cudgegong, Barrington Tops-Yarrowitch, 5 — New England fields (Inverell), 6 — Anakie fields-Rubyvale, 7 — Poona, 8 — Harts range, 9 — Lava Plains; Нигерия: 10 — Kaduna; Конго: 11 — Kinshasa; Южная Африка: 12 — Namakvaland, 13 — Barberton (Verdits); Эфиопия: 14 — Kibre mengist, Dilla; Кения: 15 — West Pokot, 16 — Baringo, 17 — Kitui, 18 — Mangare (Rockland-former John Saul mine; Penny Lane; Aqua, Hard Rock; Танзания: 19 — Umba valley; 20 — Longido, Lossogonoi, 21 — Winza; Loolera (Kibuko), 22 — Morogoro (Mwalazi; Visakazi; Nyama, Kibuko), Mahenge (Lukande; Mayote; Kitwalo; Ipango, 23 — Songea, 24 — Tunduru; Мозамбик: 25 — Montepuez (Namahumbire/Namahaca), M'sawize, Ruambeze; Зимбабве: 26 — O'Briens (Verdits); Демократическая Республика Конго: 27 — Mburi-Mayi; Мадагаскар: 28 — Andilamena, Ambodivoangy-Zahamena, Didy, Vatomandry, 29 — Andriba; Ankaratra (Antsirabe-Antanifotsy region, Soamiakatra-Ambohimandroso; Ambohibary), 30 — Ambositra, Ihosy, Zazafotsy, Ilakaka-Sakaraha; 31 — Bekily-Vohibory area (Ambatomena; Ianapera; Fotadrevo; Anavoha; Maniry; Gogogogo; Vohitany; Ejeda); Бразилия: 32 — State Santa Katerina, Byra-Velha, 33 — State Mato Grosso de Sul, 34 — State San Paulu, Itaka, 35 — State Minas Gerais, 36 — State Goias, 37 — State Bahia; Колумбия: 38 — Mercaderes-Rio Mayo; США: 39 — North Carolina (Corundum Hill; Cowee Valley; Buck Creek, Rock Creek), 40 — Cone Valley; Канада: 41 — Revelstoke, 42 — Baffin Island; Гренландия: 43 — South of Nuuk region (Fiskenasset district-Aappaluttoq); North of Nuuk (Stove; Kangerdluarssuk); Швейцария: 44 — Campo Lungo; Франция: 45 — Brittany (Champtoceaux), 46 — French Massif Central (Haut-Allier-Chantel; Peygerolles; Lozire-Aveyron-Marvejols), 47 — Vialat-du-Tarn, 48 — Pyrenees (Ariac); Испания: 49 — Alboran sea, 50 — Marrocos, 51 — Beni Bousera; Норвегия: 52 — Froland; Италия: 53 — Piedmont; Македония: 54 — Prilep; Греция: 55 — Gorgona-Xanthi, Paranesti-Drama; Таджикистан: 56 — Snezhnoe, Turakuloma, Badakhshan; Афганистан: 57 — Jegdalek, Kash; Пакистан: 58 — Hunza valley; 59 — Batakundi, Nangimali, 60 — Dir; Индия: 61 — Orissa, Kalahandi, 62 — Karnakata (Mysore), 63 — Andhra Pradesh (Salem district); Шри Ланка: 64 — Ratnapura, Polonnaruwa, Elahera; Непал: 65 — Chumar, Ruyil; Китай: 66 — Sichuan and Yannan, 67 — Qinghai, 68 — Yuan Jiang; Вьетнам: 69 — Luc Yen-Yen Bai, 70 — Quy Chau; Мьянма: 71 — Mogok, 72 — Namya, 73 — Mong Hsu; Таиланд: 74 — Chanthaburi-Trat (BoWaen, Bo NaWong, Wat Tok Phrom, Bo Rai, Nong Bon); Камбоджа: 75 — Pailin, Samlaut; Япония: 76 — Ida; Россия: 77 — Приморье, Первомайское проявление, 78 — Незаметнинское месторождение, Хабаровский край, 79 — Будунское месторождение, озеро Байкал, 80 — Тува, Хансангское проявление, 81 — Республика Саха (Якутия), Нерюга, Чайницкое месторождение, 82 — Вишневые горы; 83 — Южный Урал, Борзовская россыпь; 84 — Ильменские горы, Средний Урал, Корнилов лог, 85 — Макар-Рузь, 86 — Хитостров

and subtype II A2. Subtype II A1 is represented by metabasite-ultrabasites and gneisses (Winza, Longido (Tanzania); Andriba, Anavoha, Gogogogo. Ianapera; Fotadrevo, Maniry, Vohitany (Madagascar), Kibre mengist (Ethiopia); Kitui, Rockland-former, John Saul mine; Penny Lane (Kenya), M'sawize; Ruambeze (Mozambique); Karnataka, Orissa (India); Brittany (France), Froland (Norway); Hokitika (Australia); Makar-Ruz (Russia) and others). Subtype II A2 — marbles and calcium-silicate rocks — Jegdalek (Afghanistan); Chumar; Ruyil (Nepal), Snezhnoe, Turakuloma, Badakhshan (Tajikistan); Hunza valley, Batakundi; Nangimali (Pakistan); Mogok; Mong Hsu (Myanmar), Luc Yen-Yen Bai; Quy Chau (Vietnam), Morogoro, Mahenge (Tanzania); West Pokot (Kenya); Revelstoke (Canada), Ilmen Mountains and others).

Type IIB consists of two subtypes: subtype II B1 and subtype II B2.

Subtype II B1 includes plumbosilicates and metasomatites (Transvaal, O'Breins (Zimbabwe); Aqua; Penny lane, Rockland-John, Saul mine; Hard Rock (Kenya), Karnataka (India), Kitwalo (Tanzania); Bekily, Anavoha, Vohitany, Andilamena (Madagascar); Makar-Ruz, Hitostrov (Russia); Poona, Harts Range (Australia), Aappaluttoq; Nuuk-Stove, Kangerdluarssuk (Greenland); Corundum Hill (USA), etc.). Subtype II B2 includes metasomatized gneisses, shales, ultrabasite-basites of shire zones (Zazafotsy, Ambatomena, Ambositra (Madagascar); Nangimali formation (Pakistan), etc.). Complexes II B1 and II B2 are subjected to metamorphogenic-metasomatic processes of greenschist, amphibolite, or granulite facies conditions.

The detrital series is the most important for ruby mining. Two types belong to this series — Type IIIA and Type IIIB. Type IIIA is represented by placer deposits in the areas of alkaline basalts and kimberlites (Lava Plains, Anakie

fields, New England fields; Macquarie-Cudgegong, Barrington Tops; Tumbarumba, Western Melbourne fields (Australia); Chanthaburi-Trat (Thailand); Pailin (Cambodia); Ankaratra, Vatomandry (Madagascar) and others). Type IIIB comprises placers in metamorphic complexes (Ratnapura; Elahera, Polonnaruwa (Sri Lanka); Mogok; Mong Hsu (Myanmar); Ilakaka, Andilamena; Didy; Zahamena (Madagascar); Luc Yen, Yen Bai, Quy Chau (Vietnam); Tunduru, Songea, Winza, Umba valley, Morogoro; Mahenge (Tanzania); Montepuez; M'sawize; Ruambeze (Mozambique); Cowee Valley (USA) and others). Complexes IIIA and IIIB are unmetamorphosed.

Thus, the magmatic, metamorphogenic and detrital series of corundum-bearing formations have been identified on the basis of previous studies [4, 6, 10, 15, 16, 17, 18, 19, 20, 23, 30] and our own data [34–36].

The technological mineralogy of corundum deposits is related to the geological and tectonic position, and the specific features of regional metamorphism as applied to specific ruby-sapphire mineralization. All properties of noble corundums are determined by their primary origin. In contrast to the international classification, we propose to separate metasomatic deposits of noble corundums into two groups for their genetic typification: 1) metasomatic, which owe their origin to the action of postmagmatic hydrothermal solutions, and 2) metamorphogenic-metasomatic, genesis of which is a logical completion in local zones [34]. Identified genetic groups of ruby deposits in their geological position determine the features of structure, composition and properties of minerals more accurately, i. e., typomorphism [36]. Studies by N. G. Barnov et al. [34] place less emphasis on the position that the magmatic series includes deposits of magmatic, pegmatitic, skarn, metasomatic (postmagmatic) genesis.



As a rule, processes of allochemical metasomatism, rock desalinization and alumina enrichment of mineral-forming solutions develop on the contact of rocks of contrast composition (ultramafic and granitoids or marble and mafic), exchange of components between them, additional inflow of substance from deep Earth zones and frequent variations of chemical composition of mineral-forming solutions circulating in metasomatism zones.

Not all genetic types of ruby and sapphire deposits are equally significant for gem mining. The noble corundums of pegmatite origin have little industrial importance. They have been mined in small amounts from formations of this genetic type in India (Tamil Nadu), Brazil (Goias), Canada (Bancroft ore field, Ontario), Russia (Murzinskaya-Aduyskaya strip), but have never been considered as a promising source for industry supply.

Noble corundums are formed in the favorable environment for growth of transparent crystals, but such conditions are extremely rare in nature. For example, corundums of alkaline basic lamprophyres are crystallized from aluminum-rich magmas at deep (mantle) levels [4]. Ruby-bearing marbles and associated ruby placers are spread over a vast area of the Mogok mining district in Northern Myanmar and in several areas of Thailand. Large sapphire placers are developed in eastern Australia, Sri Lanka, Thailand and Cambodia, where their primary sources — sapphire-bearing basalts — occupy a large area.

Megacrystals of corundum in situ are rare; they are known only in basaltoids, which break through the continental crust, and confine to the areas of extensive continental uplift.

Corundum formation is a protocrystallization from melts in deep magmatic sources under the condition of subsequent rapid solidification of the main mass of the melt. Typical corundum-bearing rocks are corundum syenites and syenite-pegmatites, which form dikes and veins among alkaline syenites or granite-gneisses and gneisses near their contacts with massifs of alkaline or nepheline syenites. Examples of such include deposits of the Ilmensky and Cherry Mountains in Russia, the provinces of Ontario and Quebec in Canada, Madras and Kashmir in India, the island of Sri Lanka and others.

Corundum is formed in magmatic melt from excessive alumina, and its crystallization occurs at great depth under the condition of rapid magma ascent to the surface [12]. The features of geochemical composition of clinopyroxene and garnet megacrystals from the alluvial sapphire deposit Dac Nong (Vietnam) and model calculations showed that they were formed as a result of crystallization of alkaline basalts in a deep intermediate chamber (pressure 14–15 kbar), which is close to MOX boundary (50 km) for this part of South-East Asia [13].

The excess of alumina required for corundum crystallization, is usually fixed at the contacts of hyperbasites with dikes of acidic or basic feldspathic rocks. In such conditions, metasomatic processes play a great role. These processes develop during the desilification of aluminosilicate rocks, which contact with ultramafic rocks; at this moment, the formation of fine-, medium- and coarse-grained rocks, containing corundum, occurs. In kyshtymites, for example, the corundum content reaches 90% (Borzovskoye corundum deposit in the Urals). Corundum-containing alkaline lamprophyres are crystallized from aluminum-rich magmas at deep (mantle) levels (Yogo

Gulch deposit in Montana, USA) and Cenozoic olivine and feldspathoid alkaline basalts (Anakie deposit in Australia, Pailin in Cambodia and others); sapphire accumulations are noted in the latter.

Gem extraction from dense bedrock basalts, marble and gneisses is only possible with drilling, crushing and other technological methods, which sharply increase the cost of mining; the mining becomes unprofitable, and the extracted raw materials become defective because of the formation of numerous technogenic cracks in the crystals. Therefore, placers are generally the most important source of rubies and sapphires; gem extraction from primary, relatively soft marbles (in comparison to other rocks) is done manually and in limited quantities in Afghanistan, Pakistan, India, Myanmar, and some other countries.

Corundum is a polygenic mineral; it is widespread and found among rocks of varied composition and origin. As a rock-forming mineral, it is present in some crystalline schists and hornblendes of high degree of metamorphism, in scarny marble, in secondary quartzites, in corundum syenite-pegmatites and in plagioclases (plumasites, kyshtymites, marundites). In the form of single occurrences, corundum is found in peridotites, alkaline and nepheline syenites, granites, granite pegmatites, basalts, andesites, trachytes and other igneous rocks.

As a resistant mineral, corundum is practically unchanged in placer deposits, except for a common weak abrasion due to corundum high hardness. For this reason, all properties of noble corundums are determined by their primary origin; the physical and chemical features of rubies and sapphires and the characteristics of their main deposit types become the basis for understanding their genesis.

Research method

High-precision trace elemental analysis of original corundum samples was carried out by a quadrupole mass spectrometer X-SERIES 2 Terhmo in IGEM RAS. The results of the analysis are illustrated with the spider diagram (Fig. 2).

Electron-microscopic analysis of corundum crystals was carried out by a scanning electron microscope Carl Zeiss EVO-LS-10 equipped with energy dispersive spectrometer Oxford MAX 50. As a result, qualitative EMF spectra were obtained for a number of samples and mapping of separate areas by chemical composition was carried out.

The research was carried out with Nicolet 380 FT-IR spectrometer using a THERMO Scientific Centaurus microscope. The special feature of this equipment is the use of special OMNIC computer program necessary for automated acquisition of spectra, their quality control, as well as data analysis and processing. The sample preparation is not necessary when working with an infrared microscope. The size of the sample for analysis can be limited. The optimal particle thickness ranges from 0.005 to 0.015 mm. Centaurus infrared microscope equipped with a highly sensitive MST-A detector allows to analyse particles as small as 40 microns in the range of 600–4000 cm⁻¹ in transmission and reflection mode. Interpretation of the obtained spectra was carried out using the database and the methodology developed at CNIGRI [39].

The mineral chemical compositions were studied by an electron-probe microanalyzer JXA-8100 by JEOL in the



laboratory of mineral matter analysis of IGEM RAS. The analysis was carried out at accelerating voltage 20 kV, current on the Faraday cylinder 20 nA, probe diameter 3–5 microns. Exposure time to the main elements was 10 sec. The corrections were calculated using the ZAF correction method using JEOL software.

The surface of studied samples was polished and sprayed with a thin layer of carbon to ensure electrical conductivity.

For visual observation of fluid inclusions (FI), as well as for thermometric and cryometric studies, double-sided transparent-polished plates with 0.25–0.3 mm thickness were made from corundum samples. The area of the plates was several square centimetres.

Using Olympus BX-51 optical microscope, the shape and dimensions of PVs were determined. Microthermometric studies of PV were carried out in the sector of mineralogy of IGEM RAS by a measuring complex based on THMSG-600 microthermometer of Linkam (England).

To obtain reliable microthermometric data, a research was conducted on groups of at least two fluid inclusions with the same phase relations and close temperatures of phase transitions to ensure the initial homogeneity of the trapped fluid. The temperature measurement accuracy was ± 0.2 °C for the temperature range from –60 to +60 °C and ± 1.5 °C out of range.

Results were interpreted by standard methods [3, 24]. The composition of the main salt components of the solutions was determined by the eutectic melting point (Tevt).

Characteristics of world noble corundums

Results of high-precision trace elemental analysis (of impurities and trace elements) are shown for several selected examples of world deposits and occurrences of noble corundums from the authors' collection (fig. 2).

Table 1 shows representative analyses of corundum by genetic type from several sources.

The infrared spectra of individual micrograins in the same sample vary (Fig. 3), indicating heterogeneous composition of corundum. The spectra of transparent and translucent grains differ significantly from each other. Most of the samples show IR absorption in three spectral intervals 4000–2500 cm⁻¹, 2200–1900 cm⁻¹ and 1500–700 cm⁻¹. The last interval corresponds to natural vibrations of the crystal lattice of corundum. This conforms with the fact that only lines in the interval 1500–700 cm⁻¹ can be traced in colourless transparent corundum, containing no visible impurities (Fig. 4).

In area 4000–2500 cm⁻¹ show valence vibrations of OH- and NH-groups (Fig. 5)

In this case, hydroxyl groups are most likely to be included in adsorbed water (gas-liquid inclusions, intergranular water) as well as structural hydroxyl groups very typical for corundum. It can be assumed that clear lines near 3310, 3292, 3080 cm and some others (Fig. 5) refer exactly to valent vibrations of structural OH-groups. These groups can be considered as typomorphic properties of corundum from different deposits. Narrow lines 2120 and 1990 cm⁻¹ seem to be related to strain vibrations of structural OH-groups.

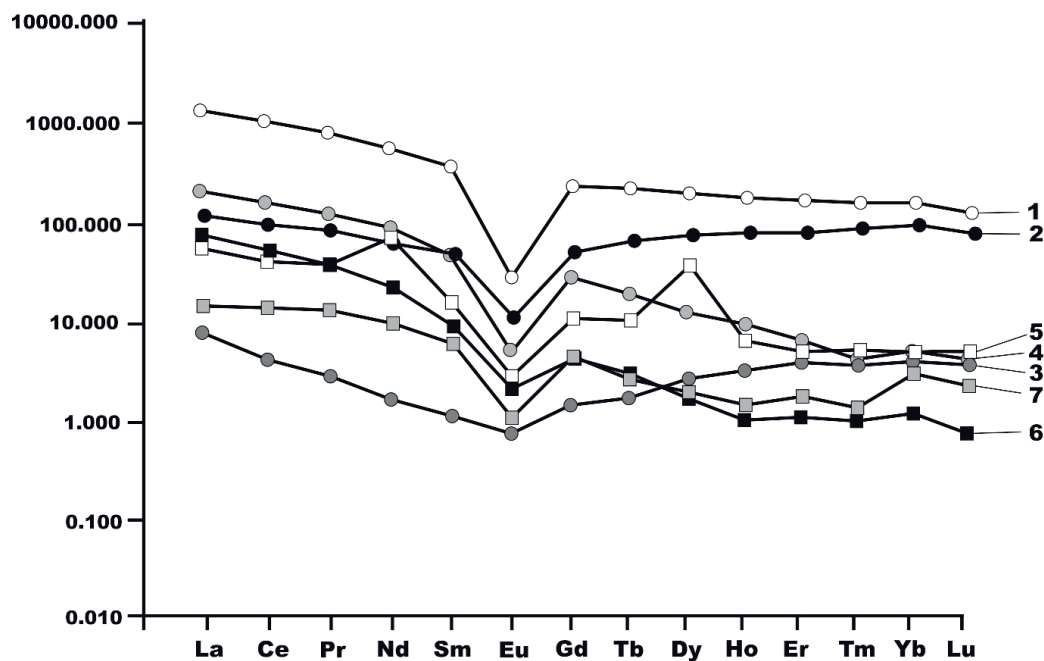


Fig. 2. Multielement spider diagram for corundum. The REE contents of corundum (ppm) are normalised to chondrite [37]. 1 — ruby in gneiss, Madagascar, subtype II B2 (assay 60); 2 — blue corundum, Olkhon island, Lake Baikal, Russia II B1 (assay 32); 3 — sapphire, Ambositra, Madagascar, subtype II B1 (assay 34); 4 — pink corundum, Morogoro, Tanzania, subtype II A2 (assay 40); 5 — corundum, Jegdalek, Afghanistan, subtype II A2 (assay 41); 6 — ruby, Karnataka, India, subtype II B1 (assay 55); 7 — corundum, India, subtype II B1 (assay 2)

Рис. 2. Мультиэлементная спайд-диаграмма для корундов. Нормализованные по хондриту [36]. Содержание элементов-примесей и РЭЭ в корундах, ppm: 1 — рубин в гнейсе, Мадагаскар, подтип II B2 (проба 60); 2 — синий корунд, остров Ольхон, оз. Байкал, Россия II B1 (проба 32); 3 — сапфир, Амбоситра, Мадагаскар, подтип II B1 (проба. 34); 4 — розовый корунд, Морогоро, Танзания, подтип II A2 (проба 40); 5 — корунд, Джегдалек, Афганистан, подтип II A2 (проба 41); 6 — рубин, Карнатака, Индия, подтип II B1 (проба 55); 7 — корунд, Индия, подтип II B1 (проба 2)

Table 1. Representative oxide analyses (wt %) of EMPA rubies originating from deposits of different geological types according to the new improved geological classification for ruby

Таблица 1. Репрезентативные анализы оксидов (мас. %) EMPA рубинов, происходящих из месторождений различных геологических типов, в соответствии с новой, усовершенствованной геологической классификацией для рубина

Type of deposit Тип место- рождения	Deposit Место- рождение	Colour corundum Цвет корунда	Country Страна	Al ₂ O ₃	MgO	TiO ₂	V ₂ O ₃	Cr ₂ O ₃	FeO	Ga ₂ O ₃	Total Всего	References Ссылки
Type IA	Somiakatra	deep red	Madagascar	98.16	na	0.03	0.060	0.858	0.52	0.01	99.64	29
		pink		98.75	na	0.01	0.000	0.243	0.26	0.01	99.28	
Type IB	MbuijiMayi	fushsia	RDC	93.76	0/01	0.01	0.029	5.641	0.47	0.01	99.94	9
	Paranesti	red	Greece	97.58	bdl	0.01	0.010	2.650	0.39	0.07	100.71	32
Type IIA ₁	Montepuez	red	Mosambique	99.38	bdl	0.01	na	0.080	0.45	bdl	99.92	5
	Vohitany	red	Madagascar	99.06	0.01	0.01	0.010	0.219	0.59	0.01	99.90	6
	LucYen	red to pink	Vietnam	99.42	0.02	0.02	0.10	0.370	0.02	0.01	99.90	20
	Nanggimali	pink	Pakistan	99.85	0.01	0.02	0.050	0.055	0.00	0.01	99.88	6
Type IIB ₂	Anovoha	pink	Madagascar	98.76	0.00	0.00	0.020	0.023	0.45	0.00	99.85	6
	Zazafotsy	red	Madagascar	98.63	0/01	0.03	0.005	0.188	0.30	0.01	99.17	6
	Hokitika	red	New Zeland	90.65	na	bdl	0.050	9.050	0.18	na	99.93	11
		red		98.43	0.02	0.04	0.040	0.761	0.52	0.02	99.83	28
Type IIIB	Vatomandry	red brown	Madagascar	99.50	0.03	0.02	0.012	0.127	0.21	0.01	99.91	7
	Macquarie	red	Australia	99.07	0.09	bdl	na	0.450	0.22	na	99.83	29
	Quy Chau	red to pink	Vietnam	99.28	0.00	0.03	0.020	0.580	0.06	0.01	99.98	20
	Luc Yen	red to pink		99.76	0.00	0.01	0.070	0.540	0.01	0.01	100.40	20

Note: na – not analyzed, bdl – below detection limit.

Примечание: na – не проанализировано, bdl – ниже предела обнаружения.

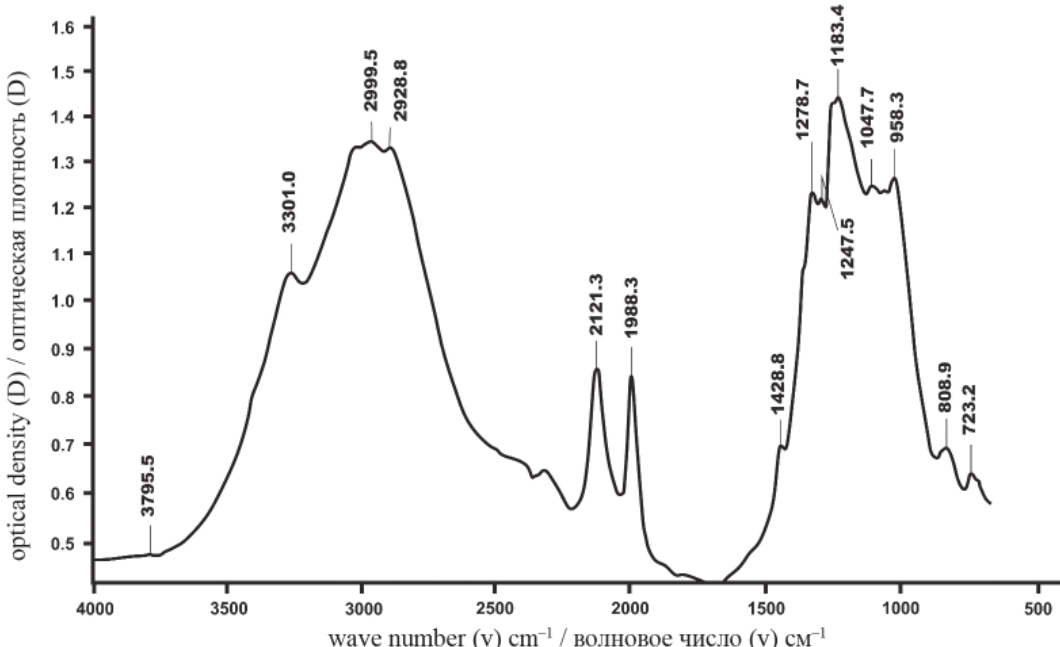


Fig. 3. Infrared spectrum of leucosapphire (sample 34 – Ambositra, Madagascar, subtype II B2)

Рис. 3. ИК-спектр лейкосапфира (обр. 34 – Амбоситра, Мадагаскар, подтипа II B2)

A number of examples are illustrated in Figs. 6, 7, 8, 9.

Minerals were studied by an electron-probe micro-analyser in the Mineral Analysis Laboratory of IGEM RAS. Corundum and silicate phases were analysed using the following standards:

Si – sanidine, Na – jadeite, Fe – almandine, K – sanidine, Ni – NiO, Al – corundum, Mg – olivine, Mn –

spessartine, Ca – anorthite, Cr – chromite, Ti – titanite. During the analysis of ore inclusions the standards: Ti – ilmenite, Mg – chromite, Fe – magnetite, Ca – sphene, Ni – Ni, Si – almandine, Mn – spessartine, Nb – Rb₂Nb₄O₁₁, V – V, Cr – chromite, Al – chromite were used. For single zircon inclusions the following references were used: Si – zircon, P – apatite, Zr – zircon, U –

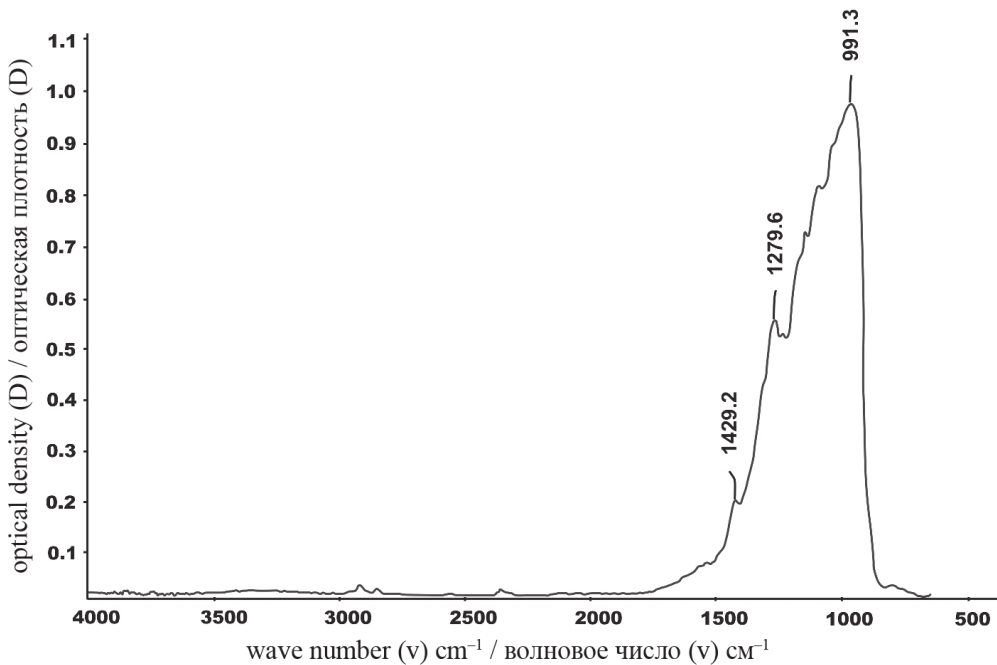


Fig. 4. Infrared spectrum of ruby (sample 2, deposit Snezhnoe, Tajikistan, subtype II A2)

Рис. 4. ИК-спектр рубина (обр. 2, месторождение Снежное, Таджикистан, подтип II A2)

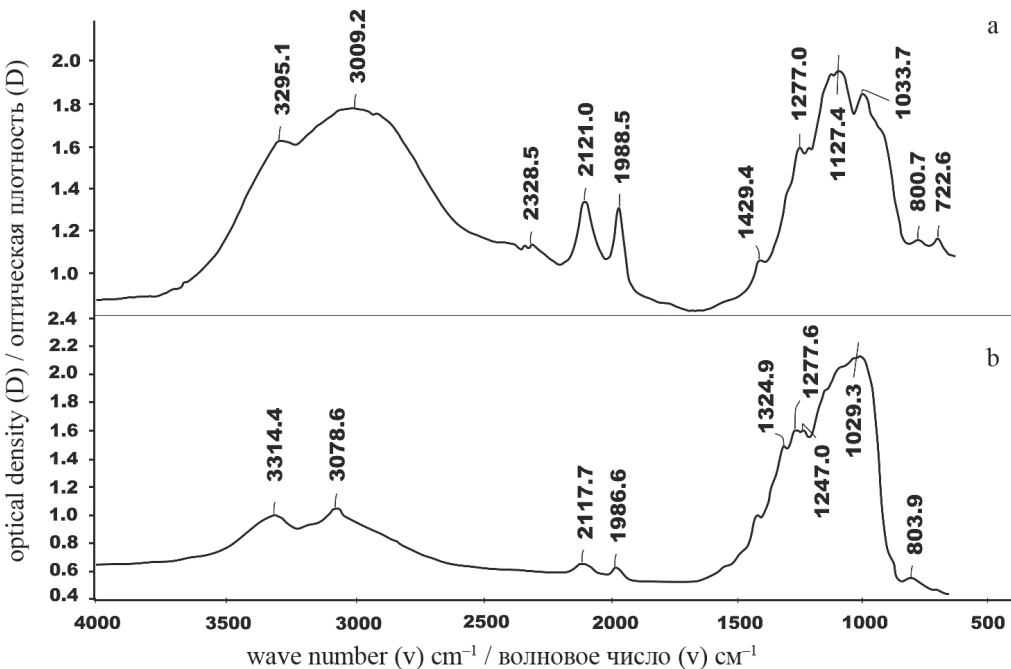


Fig. 5. IR spectrum of light corundum (sample 26/15 – Hunza, Pakistan, II A2)

Рис. 5. ИК-спектр светлого корунда (обр. 26/15 – Хунза, Пакистан, II A2)

UO₂, Hf – HfO₂, Y-Y₂O₃, Th- ThPO₄, S – BaSO₄, Nb – Rb₂Nb₄O₁₁.

Mineral inclusions are represented by magnetite, zircon, amphibole, mica, chlorite, apatite, rutile, ilmenite and rare earth minerals. Study materials by electron-probe microanalyzer JXA-8100 from company JEOL are shown on Figs. 10, 11, 12, 13, 14.

In some samples the impurities of elements-chromophores, iron, chromium and titanium, were noted.

Indexes: Crn – corundum, Dsp – diaspore, Rt – rutile, Grt – garnet, Pl – plagioclase, Ap – apatite, Mc – microcline, Zrn – zircon, Chl – chlorite, Pcl – pyrochlore, Ms – muscovite, Kln – kaolinite, Mag – magnetite,

Among the FS, the following are highlighted: the first group – FS, which occur singly or form chaotic irregular clusters in the central parts and sometimes at the edges of the grains. Sometimes these fluid inclusions are confined to crystal growth zones; the second group – FS forming chains and planes, confined to cracks crossing several grains.

According to the criteria of E. Roedder [22], the first group of inclusions is referred to the primary, trapped during the crystal growth, the second group is referred to the secondary, which contain the fluid penetrated through cracks after crystallization of the mineral. The size of primary inclusions is from 2 to 50 microns; inclusions have

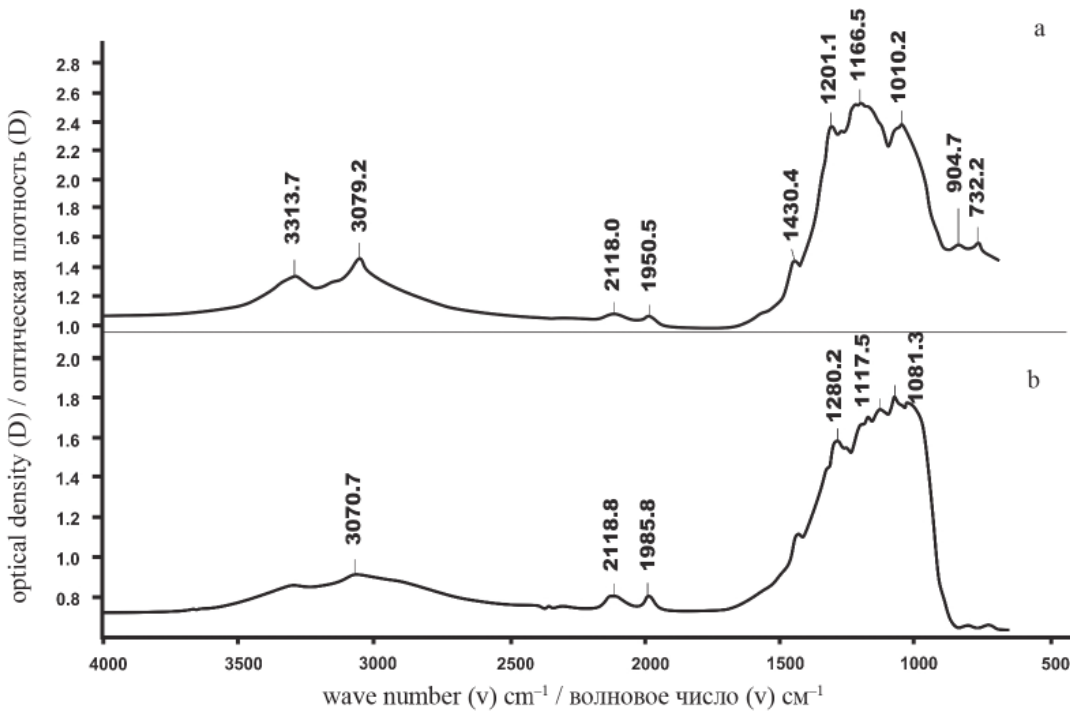


Fig. 6. IR spectrum of ruby (sample 1 — Longido, Tanzania, II A1)

Рис. 6. ИК-спектр рубина (обр. 1 — Лонгидо, Танзания, II A1)

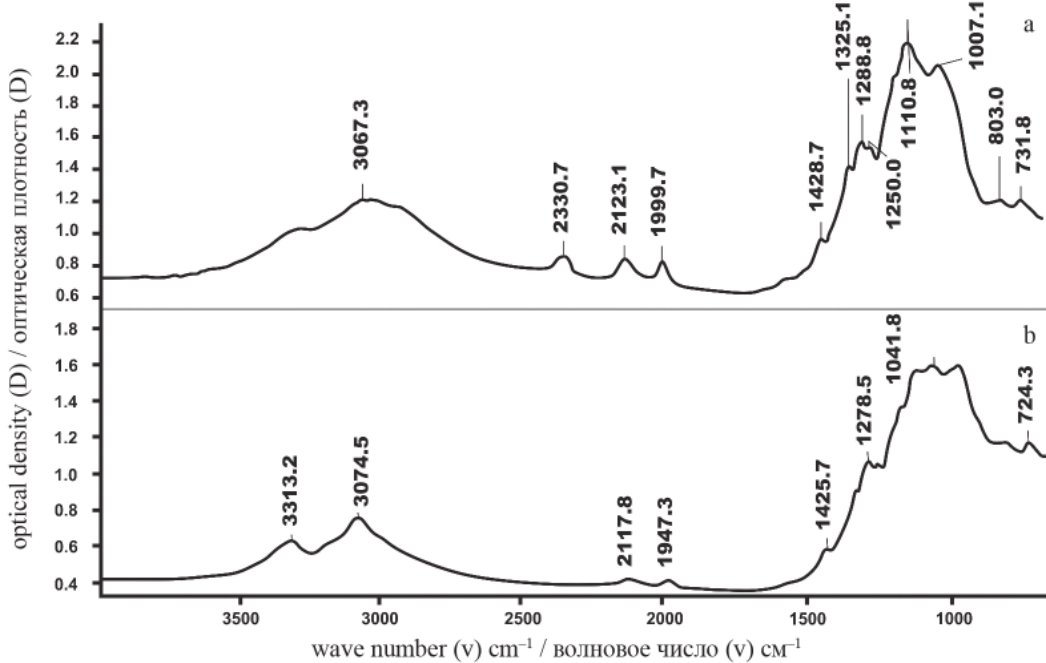


Fig. 7. IR spectrum of pink corundum (sample 40 — Morogoro Circle 40, Tanzania, II A2)

Рис. 7. ИК-спектр розового корунда (обр. 40 — Морогоро, Танзания, II A2)

rounded elongated or irregular shape or shape of negative crystals with elements of crystallographic cut. The size of secondary inclusions does not exceed 10 μm . Primary fluid inclusions with sizes from 5 μm and, in some cases, large secondary inclusions (from 5 μm) have been selected for the study.

According to the phase composition at room temperature all inclusions are single-phase. On cooling and heating it was found that all PVs contain liquid carbonic acid. List of the main samples analysed (No. 3 Musse, Kashmir, India (blue No. 29, Zapskor, Kashmir; No. 47 ruby, Mysore,

Karnataka State, India; No. 4 Mura-Bora, Tanzania, No. 5 Ihosy, No. 40 pink corundum, Morogoro; No. 48 ruby in muscovite, Moro Goro, Tanzania; Madagascar (pegmatite); No. 7 Olkhon Island, Baikal, Russia; No. 10, Rai-Iz, Polar Urals, Russia; No. 19 Ilmensky Nature Reserve, Urals, Russia; No. 20 Budun on Olkhon, Baikal; No. 32 blue corundum, Olkhon Island, Baikal, Russia; No. 23 Ihosy; No. 30 Vatondradi, No. 34 leucosapphire, Ambusitra, Madagascar; No. 36 Sandnessien, Norway; No. 38 blue corundum, Koltashi village, Middle Urals, Russia; No. 39 corundum, Muzor, India.

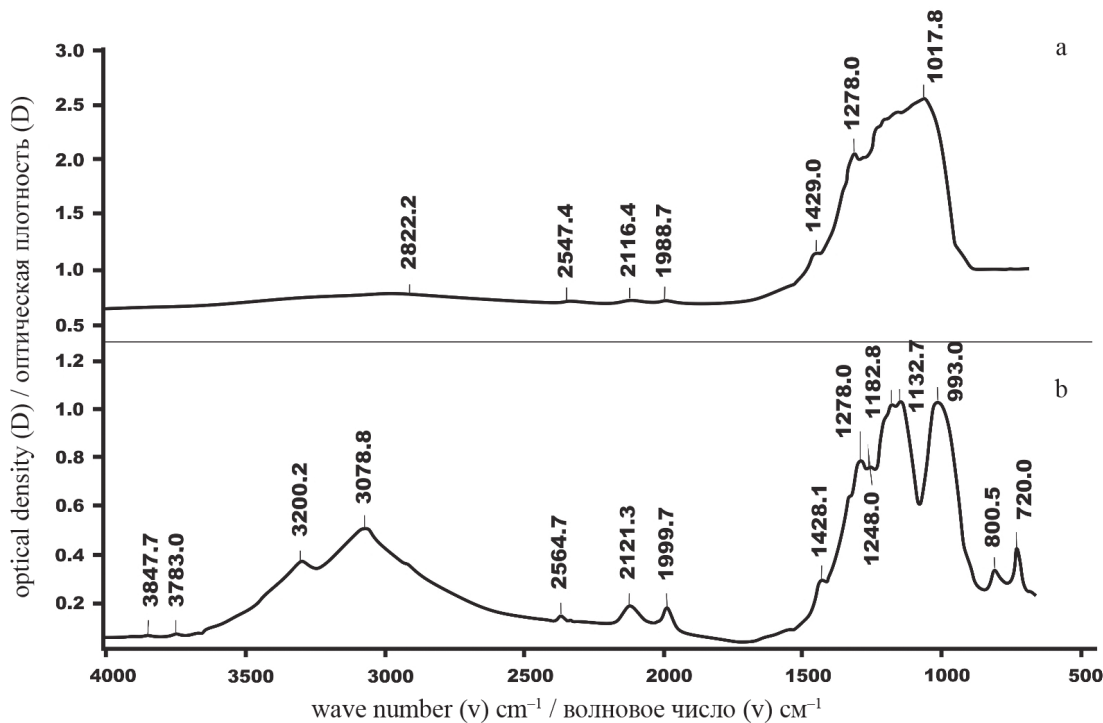


Fig. 8. IR spectrum of corundum (sample 44, Luc Yen-Yen Bai province, Vietnam, II A2)

Рис. 8. ИК-спектр корунда (обр. 44, провинция Лук Йен-Йенбай, Вьетнам, II A2)

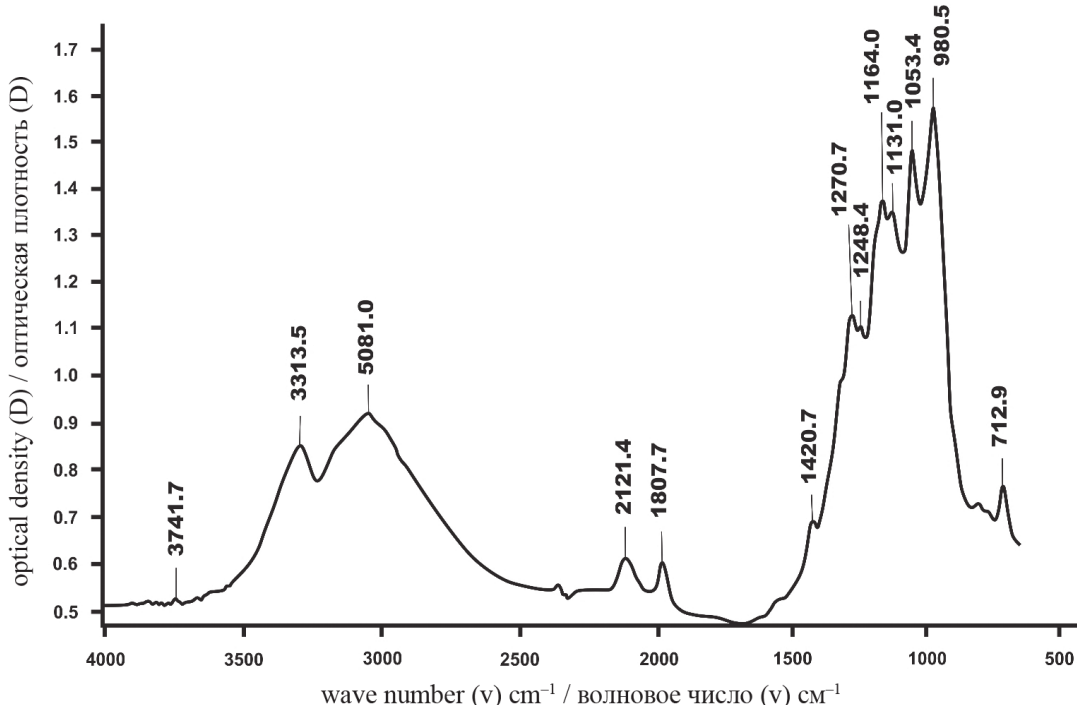


Fig. 9. IR spectrum of ruby (sample 53, Khitostrov, Karelia, Russia, II B1)

Рис. 9. ИК-спектр рубина (обр. 53, Хитостров, Карелия, Россия, II B1)

Two-phase PVs — gas + liquid — have been found in some corundums. According to the ratio of phases in them 2 types can be distinguished: 1 — with the gas phase occupying not more than 30 % of PV volume; 2 — with the gas phase occupying up to 50 % of PV volume. Fluid inclusions of the first type contain water-salt fluid. Fluid inclusions of the second type contain carbon dioxide-methane fluid.

The crystallization of all corundums was likely to occur in a heterogeneous medium consisting of immiscible

low-salinity water-salt and high-density carbonic acid fluids. The inclusions of the first type occur in chains and planes next to chains of inclusions of the second type (carbonic acid), which suggests their syngensis, i.e., simultaneous trapping.

High-density carbonic acid with small amounts of other gases was the predominant component of the mineral-forming system during corundum crystallization. The amount of impurities (methane) in the inclusions varies from 12 to >1 % [7].

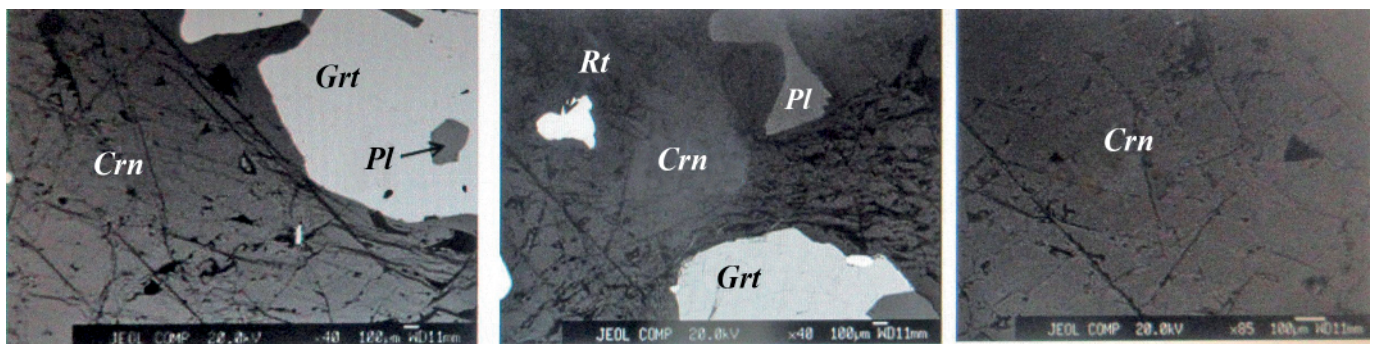


Fig. 10. Back-scattered electron (BSE) images. Mineral inclusions in corundum (sample 14 – corundum, Jegdalek, Afghanistan)
Рис. 10. Back-scattered electron (BSE) images. Минеральные включения в корунде (обр. № 14 – корунд, Jegdalek, Афганистан)

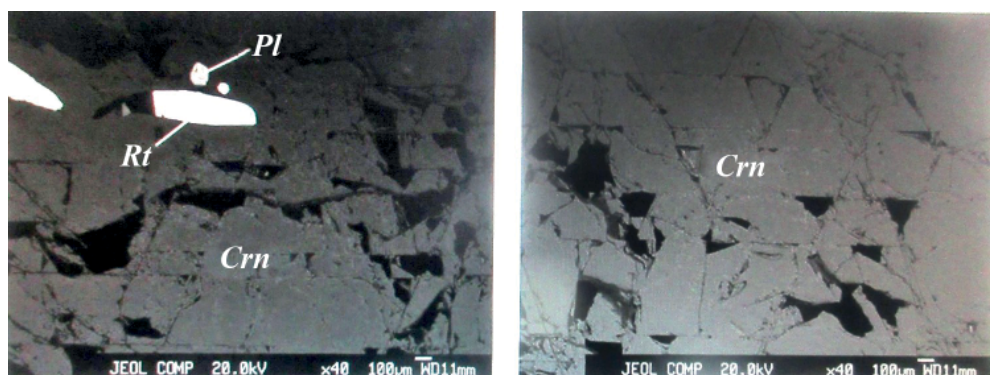


Fig. 11. Figure 11 Back-scattered electron (BSE) images. Mineral inclusions in corundum (sample 6 Karnataka, Mysore district, India)

Рис. 11. Back-scattered electron (BSE) images. Минеральные включения в корунде (обр. № 6 Karnataka, Mysore district, Индия)

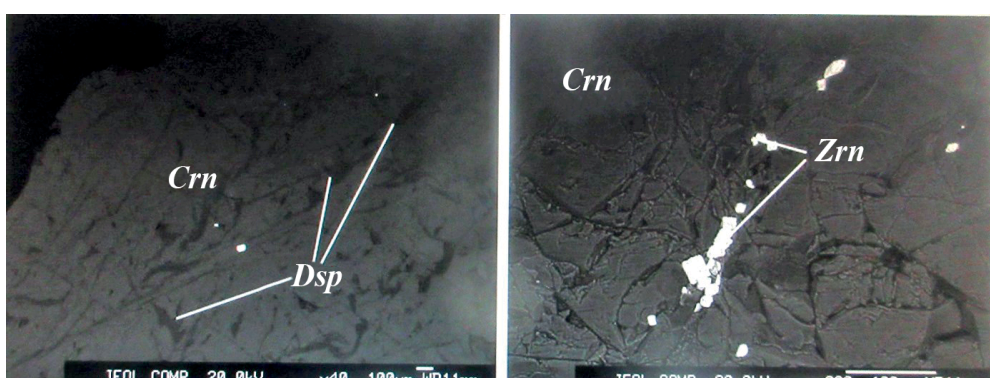


Fig. 12. Back-scattered electron (BSE) images. Mineral inclusions in leucosapphire (sample 34 Ambositra, Madagascar)
Рис. 12. Back-scattered electron (BSE) images. Минеральные включения в лейкосапфире (обр. № 34, Ambositra, Мадагаскар)

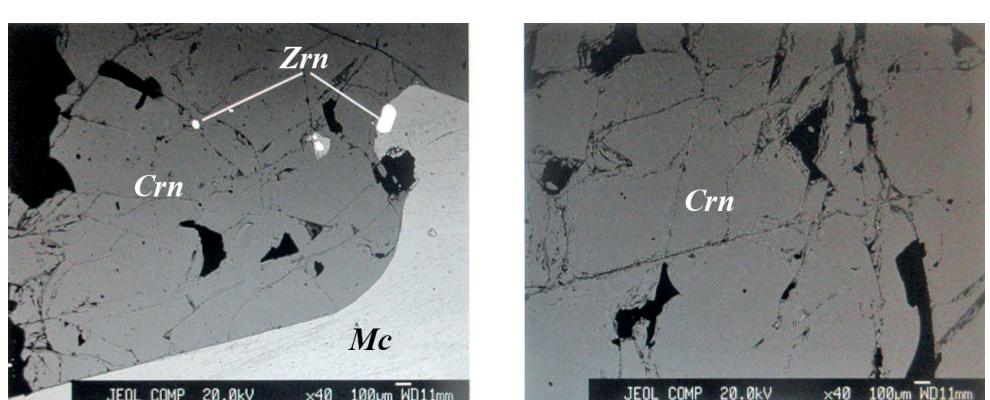


Fig. 13. Back-scattered electron (BSE) images. Mineral inclusions in sapphire (sample 23 Ihosy, Madagascar)

Рис. 13. Back-scattered electron (BSE) images. Минеральные включения в сапфире (обр. № 23, Ihosy, Мадагаскар)

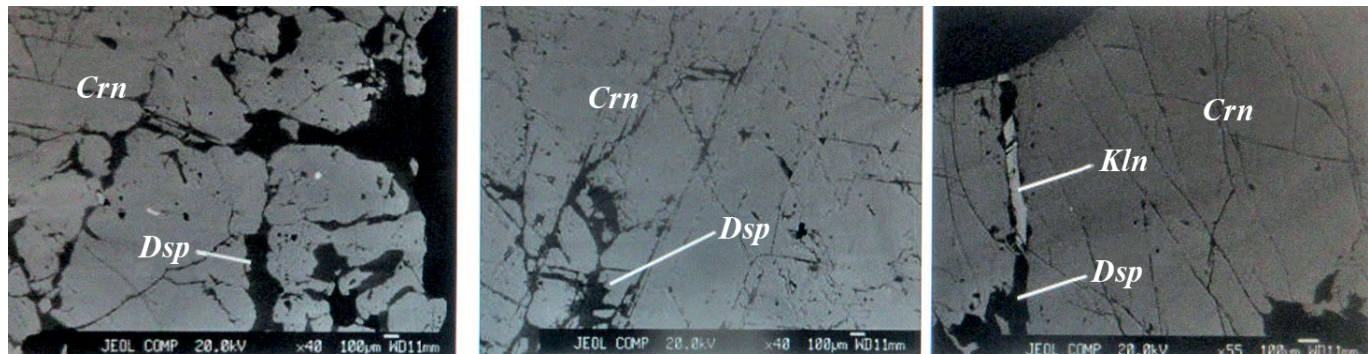


Fig. 14. Back-scattered electron (BSE) images Mineral inclusions in corundum
(sample 44, Luc Yen-Yen Bai province, Vietnam)

Рис. 14. Back-scattered electron (BSE) images. Минеральные включения в корунде
(обр. № 44, провинция Лук Йен-Йенбай, Вьетнам)

Main applications for corundum, rubies and sapphires

- for grinding precious stones, metals and optical glasses
- manufacturing of grinding machine wheels from cemented ground corundum sandpaper
- rubies are used as bearings and backstones in watch movements, ensuring high precision and prolonging their life. Up to 16 of these can be fitted in a single watch movement.
- sapphire is used to produce a superstrong glass known as sapphire crystal.
 - sapphire crystal is popular for mobile phones
 - rubies and sapphires are used in optical quantum generators (lasers)
 - sapphire does not react with any acids and alkalis, resists high pressures and temperatures, harsh radioactive radiation
 - sapphire windows in devices and apparatuses where vacuum, high temperatures and pressures reign, bathyscaphes etc.
 - sapphire as a differential pressure sensor is used to detect emergency sections of gas pipelines
 - a millimeter-long layer of corundum insulators replaces a five-centimeter-long layer of ordinary mineral wool
 - corundum is a unique type of fibre-reinforced high-performance cement composite, which fulfills the highest requirements for new roads.

Conclusion

The systematisation and synthesis of available material and our own data on noble corundum deposits around the world provide an opportunity to assess the role of indigenous corundum-bearing objects in the geological history of their formation.

The first group includes primary deposits of magmatic, pegmatitic and metasomatic (postmagmatic) origin, and the second — includes polychronous and polyfacial primary metamorphic and metamorphogenic-metasomatic deposits.

Deposits of metamorphogenic type are generally older than deposits of other types. Their age is defined as Archean in Greenland, Neo-Archean-Paleoproterozoic in Russia (Karelia, etc.), South Asia (India, Sri Lanka, Myanmar,

Tajikistan, etc.) and East Africa (South Africa, Madagascar), Proterozoic in the USA (North Carolina) and Upper Paleozoic, and sometimes even older in Southern Russia, Africa, Asia and Australia (Ural, Kenya, Tanzania, Mozambique, etc.).

The analysis of the geological position and genesis of noble corundum deposits allows us to interpret the properties of rubies and sapphires and to recommend their use in traditional and special, including fundamental diagnostics.

The work was supported by the R&D project 210 IG KarSC RAS 121040600173-1

References

1. Andersen B. W. Payne G. J. The constancy of quartz and other minerals. *Gemmologist*, 1940, No. 9, 93 p.
2. Arlabosse, J.-M., Delaunay, A., Lenne, N. Les rubis de Vatomandry. *Madagascar. Rev. Ass. Fr. Gemmol.*, AFG2018, 203, pp. 6–15.
3. Bodnar, R. J., Vityk M. O. Interpretation of Microthermometric Data for H₂O-NaCl Fluid Inclusions. In: De Vivo, B. and Frezzotti, M. L., Eds., *Fluid Inclusions in Minerals: Methods and Application*. Pontignano-Siena, 1994, pp. 117–130.
4. Brownlaw, A. H., Komorowsky J-C. Geology and origin of the Yogo sapphire deposit, Montana. *Economic Geology*, 1988, 83(4), pp. 875–880.
5. Fanka, A.; Sutthirat, C. Petrochemistry, mineral chemistry, and pressure-temperature model of corundum-bearing amphibolite from Montepuez, Mozambique. *Arab. J. Sci. Eng.* 2018, 43, pp. 3751–3767.
6. Giuliani G., Groat L., Fallick A., Pignatelli I. and Pardieu V. Ruby Deposits: A Review and Geological Classification. *Mineralogy and Geochemistry of Ruby. Minerals*, 2020, 10, 597, pp. 11–93. DOI:10.3390/min10070597.
7. Giuliani, G.; Fallick, A. E.; Rakotondrazafy, A. F. M.; Ohnenstetter, D.; Andriamamonjy, A.; Rakotosamizanany, S.; Ralantsoarison, T.; Razanatseheno, M. M.; Dunagre, C.; Schwarz, D. Oxygen isotope systematics of gem corundum deposits in Madagascar: Relevance for their geological origin. *Mineral. Depos.*, 2007, 42, pp. 251–270. DOI:10.1007/s00126-006-0105-3.
8. Giuliani, G.; Ohnenstetter, D.; Fallick, A. E.; Groat, L.; Fagan, J. The geology and genesis of gem corundum deposits. In: *Geology of Gem Deposits*; Groat, L. A., Ed.; Mineralogical Association of Canada: Tucson, AZ, USA, 2014; Short Course Series; V. 44, pp. 29–112.



9. Giuliani, G.; Pivin, M.; Fallick, A. E.; Ohnenstetter, D.; Song, Y.; Demaiffe, D. Geochemical and oxygen isotope signatures of mantle corundum megacrysts from the Mbui-Mayi kimberlite, Democratic Republic of Congo, and the Changhe alkali basalt, China. *C.R. Geosciences*, 2015, 347, pp. 24–34.
10. Graham, I.; Sutherland, L.; Khin, Z.; Nechaev, V.; Khanchuk, A. Advances in our understanding of the gem corundum deposits of the West Pacific continental margins intraplate basaltic fields. *Ore Geol. Rev.*, 2008, 34, pp. 200–215.
11. Grapes, R.; Palmer, K. (Ruby-sapphire)-chromian mica-tourmaline rocks from Westland, New Zealand. *J. Petrol.* 1996, 37, pp. 293–315.
12. Guo, J., O'Reilly, S. Y., Griffin, W.L. Corundum from basaltic terrains: a mineral inclusion approach to the enigma. *Contr. Miner. Petrol.*, 1996, V. 122, pp. 368–386.
13. Hong-sen X., Wei-guo Z., Wei H., Wen-ge Z., Jie G., Jian X. Discovery of corundum in alkali basalt at high temperature and high pressure. *J. Physics, Condensed Matter*, 2002, V. 14, pp. 11365–11368. DOI:10.1088/0953-8984/14/44/483
14. Hughes R. W. *Ruby & Sapphire*. RWH Publishing, 1997, 512 p.
15. Hughes, R. W., Manorotkul, W. & Hughes, E. B. *Ruby & Sapphire: A Gemologist's Guide*. Lotus Publishing, 2017, Bangkok, 816 p.
16. Hutchinson, M. T.; Nixon, P. H.; Harley, S. L. Corundum inclusions in diamonds-discriminatory criteria and a corundum composition dataset. *Lithos*, 2004, 77, pp. 273–286. DOI:10.1016/J.LITHOS.2004.04.006.
17. Iyer, L. A. N. The geology and gemstones of the Mogok stone tract, Burma. *Memoirs of the Geological Survey of India*, 1953, V. 82, pp. 7–100.
18. Jons, N., Schenk, V. Relics of the Mozambique Ocean in the central East African Orogen: Evidence from the Vohibory Block of Southern Madagascar. *J. Metam. Geol.*, 2008, 26, pp. 17–28.
19. Keulen, N.; Thomsen, T. B.; Schumacher, J. C.; Poulsen, M. D.; Kalvig, P.; Vennemann, T.; Salimi, R. Formation, origin and geographic typing of corundum (ruby and pink sapphire) from the Fiskensasset complex, Greenland. *Lithos*, 2020, pp. 36–367. DOI:10.1016/j.lithos.2020.105536.
20. Nam, N. V.; Minh, N. T.; Thuyet, and Nguy Tuyet Nhung, T. N. T.; Khoi, N. N.; Suthirat, C.; Tuan, D. A. Ruby and sapphire from the Than-Huong-Truc Lau area, Yen Bai province, Northern Vietnam, *Gems & Gemology*, 2011, pp. 182–195 DOI:10.5741/GEMS.47.3.182.
21. Pham, V. L.; Hoang, Q. V.; Garnier, V.; Giuliani, G.; Ohnenstetter, D. Marble-hosted ruby from Vietnam. *Can. Gemmol.* 2004, 25, pp. 83–95.
22. Pignatelli, I.; Giuliani, G.; Morlot, C.; Pham, V. L. The texture and chemical composition of trapiche ruby from Khoan Thong, Luc Yen mining district, northern Vietnam. *J. Gemmol.* 2019, 36, pp. 726–745.
23. Rakotosamizanany, S.; Giuliani, G.; Ohnenstetter, D.; Rakotondrazafy, A.F.M.; Fallick, A.E.; Paquette, J.-L.; Tiepolo, M. Chemical and oxygen isotopic compositions, age and origin of gem corundums in Madagascar alkali basalts. *J. S. Afr. Earth Sci.* 2014, 94, pp. 156–170.
24. Roedder, E. Fluid Inclusions. Systematics of Fluid Inclusions in Diagenetic Minerals. *Mineralogical Society of America*, 1984, V. 12, 644 p.
25. Saul J. M. A Geologist Speculates: On Gemstones, Origins of Gas and Oil, Moonlike Impact Scars on the Earth, the Emergence of Animals and Cancer. Second edition, online version, ©John M. Saul, 2015, 160 p. DOI:10.1080/00357529.2016.1172181.
26. Simonet, C.; Fritsch, E.; Lasnier, B. A classification of gem corundum deposits aimed towards gem exploration. *Ore Geol. Rev.* 2008, 34, pp. 127–133. DOI:10.1016/J.OREGOREV.2007.09.002.
27. Smirnov S. Z., Izokh A. E., Kovayzin S. V., Mashkovtsev R. I., Trang Trong H., Ngo Thi P., Kalinina V. V., Pospelova L. N. Inclusions in Dak Nong placer sapphires, Central Vietnam: conditions of corundum crystallization in the continental crust. *J. Geol., Series B*, 2006, V. 28, pp. 58–70.
28. Sutherland, F. L.; Coenraads, R. R.; Abduriyim, A.; Meffre, S.; Hoskin, P. W. O.; Giuliani, G.; Beattie, R.; Wuhrer, R.; Sutherland, G.B. Corundum (sapphire) and zircon relationships, Lava Plains gem fields, NE Australia: Integrated mineralogy, geochemistry, age determination, genesis and geographic typing. *Mineral. Mag.*, 2015, 79, pp. 545–581.
29. Sutherland, F. L.; Coenraads, R. R.; Schwarz, D.; Raynor, L. R.; Barron, B. J.; Webb, G. B. Al-rich diopside in alluvial ruby and corundum-bearing xenoliths, Australian and SE Asian basalt field. *Mineral. Mag.*, 2003, 67, pp. 717–732. DOI:10.1180/0026461036740129.
30. Sutherland, F. L.; Khin, Z.; Meffre, F.; Thompson, J.; Goemann, K.; Kyaw, T.; Than, T. N.; Mhod, Z. M.; Harris, S. I. Diversity in ruby chemistry and its inclusions: Intra and intercontinental comparisons from Myanmar and Eastern Australia. *Minerals*, 2019, 9, 28 p. DOI:10.3390/min9010028.
31. Thomhson, S. R. British Tertiary volcanic province. *Scott. J. Geol.*, 1982, V. 18, pp. 49–107.
32. Voudouris, P.; Mavrogonatos, C.; Graham, I.; Giuliani, G.; Melfos, V.; Karampelas, S.; Karantoni, V.; Wang, K.; Tarantola, A.; Khin, Z.; et al. Gem Corundum deposits of Greece: Geology, mineralogy and genesis. *Minerals*, 2019, pp. 9–49. DOI:10.3390/min9010049.
33. Yui Tzen-Fu, Wu Chao-Ming, Limtrakun P., Sricharn W. Oxygen isotope studies on placer sapphire and ruby in the Chanthaburi-Trat alkali basaltic gemfield, Thailand. *Lithos*, 2006, V. 86, pp. 197–211. DOI:10.1016/J.LITHOS.2005.06.002.
34. Barnov N. G., Melnikov E. P. *Geneticheskie tipy blagorodnykh korundov* (Genetic types of noble corundum). Mining Information and Analytical Bulletin, No. 6, pp. 79–85.
35. Barnov N. G., Melnikov E. P., Victorov M. A. *Mineralogiya mestozhdenii blagorodnykh korundov mira* (Mineralogy of noble corundum deposits of the world). *Otechestvennaya geologiya*, 2016, No. 1, pp. 39–45.
36. Barnov N. G., Shchiptsov V. V. *Typologiya rubinov i ikh promyslennoe znachenie* (Typology of rubies and their industrial significance). Mining industry, No. 6, pp. 127–132.
37. Kievlenko E. Ya. *Poisky i otsenka mestorozhheniy drag-sennykh I podelochnykh kamney* (Search and evaluation of deposits of precious and ornamental stones). Moscow: Nedra, 1980, 160 p.
38. Kievlenko E. Ya., Chuprova V. I., Dramcheva E. E. *Decorativnye i kollektionskiye mineraly* (Decorative collection minerals). Moscow: Nedra, 1987, 223 p.
39. Khachatryan G., Kryazhev G. K. *Metody analiza porodo-obrazuyushchikh aktsessornykh minerelov rudnykh mestorozhdeniy s ispolzovaniem IK-Fure microscope* (Method of analysis of rock-forming and accessory minerals of ore deposits using IR-Fourier microscope). Ores and metals, 2010, No. 5, pp. 64–73.
40. Rossovsky L. N., Konovalenko S. I., Ananov S. A. *Usloviya obrazovaniya rubina v mramorakh* (Conditions for the formation of ruby in marbles). *Geology of ore deposits*, 1982, No. 2, pp. 57–66.

Received / Поступила в редакцию 09.08.2022